TRAJECTORY AND OPTICAL PARAMETERS IN A NON-LINEAR STRAY FIELD

D. Manglunki, M. Martini, CERN, Geneva, Switzerland
I. Kirsten, Heidelberg University, Heidelberg, Germany

ABSTRACT

A new optics for the main CERN Proton Synchrotron (CPS) magnet is modeled to allow a precise description of the ejected beams. For that purpose, field maps of the magnet have been measured for the various operational current settings. They include the central field, the end stray field and the lateral stray field. In order to get a functional form which can be inserted in the equations of motion for a charged particle in a magnetic field, the discrete field maps are converted into bi-dimensional polynomials of degree up to fourteen. These equations can be written as a set of four first order differential equations which are solved simultaneously. Two of them are non-linear and describe the centroid motion, the other two are linear and apply to the betatron motion. The method has been validated by producing extraction conditions which have been verified experimentally with the 26 GeV/c beam for the future LHC.

1. INTRODUCTION

The proton beams extracted from the CPS experience the strongly non-linear stray field from the magnet unit downstream of the ejection septum. Previous calculations modelled each half-magnet multipole component beyond the sextupole order as a thin element. Multipole coefficients were derived from field measurements at a reference azimuthal magnet location using one-dimensional transverse fitting. The approach considered in this paper consists integrating the equations of motion for a single proton travelling through a measured discrete field map converted into bi-dimensional polynomials. The results yield the ejection trajectory and the transfer matrices through the field map.

This study considers the ejection of a 26 GeV/c proton beam which will be used to fill the LHC [1]. The same approach could similarly be used to handle the other ejection settings (e.g. 24 GeV/c proton slow extraction) and the 1 GeV proton injection in the CPS.

2. FITTING OF FIELD MEASUREMENTS

2.1 Measured field map on a test magnet unit

The CPS lattice consists of ten super-periods made of ten combined function magnets, eight 1.0 m and two 2.4 m straight sections. Each magnet is composed of two half-units with gradients of opposite sign, separated by a central junction. The half-units are made of five blocks with small gaps in between lined up on the central orbit.

Corrections have been installed on the pole profile to create independent multipole fields: (i) pole-face windings yielding quadrupolar and sextupolar components to adjust the tunes and chromaticities modified by saturation; (ii) a figure-of-eight loop to modify the field distribution between the two half-units, allowing additional tune changes without affecting chromaticities. The various magnet settings are characterized by their dipole field level specified by the main coil current and their pole-face winding and figure-of-eight loop currents. The layout of the CPS magnet number 16 is shown in Fig. 1.

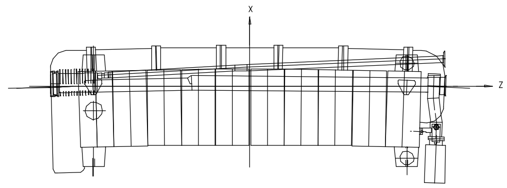

Fig. 1: CPS magnet unit number 16 including the 26 GeV/c extraction pipe.

New magnetic measurements on operational CPS magnet working points were performed in 1992, including measurements of the central field, the end and lateral stray fields, and the field in the junction between the two half-units [2]. The measured magnet unit was a radially defocusing open half-unit (D half-unit) followed by a radially focusing closed half-unit (F half-unit), with the yoke oriented towards the centre of the ring.

Measurements were carried out in a Cartesian frame with steps of 20 mm along the z-axis (aligned along the two magnet targets and counted positively in the proton direction) and steps of 10 mm along the x-axis (put in the middle of the central magnet junction and counted positively towards the outside ring). The field map range is: -70 mm $\le x \le$ 310 mm and -2.55 m $\le z \le$ 2.73 m (the magnet length is 4.26 m).

2.2 Functional form of the discrete field map

The necessity to extract a 26 GeV/c proton beam in a 2.4 m straight section with little angle deflection (≅29 mrad) imposes that the downstream half-unit adjacent to the ejection septum to be open to allow the fitting of the extraction pipe across the magnet aperture. The ejection trajectory in this region remains close to the central orbit and thus the aberrations in the magnetic fields are kept at a reasonable value. When traversing the subsequent F half-unit the ejection trajectory moves away from the central orbit and field aberrations become strongly non-linear: the beam experiences a field gradient with a reverse sign, yielding large horizontal betatron function values at the magnet end. Reduction of the non-linear aberrations was done by shimming the F half-unit. Straight parallel shims have been mounted at different radial positions on the five blocks to shape a constant magnetic field over the ejected beam width [3].

Magnetic measurements have been done on a laboratory magnet unit in the absence of shims, thus the measured field map has to be corrected to consider the shimming effect. Field calculations have been carried out on the five blocks equipped with shims using the two-dimensional Poisson program [4] with appropriate meshing of the field region [5]. Polynomial fittings up to degree twenty-five in x (in the range -0.1 m $\le x \le$ 0.5 m) of Poisson output have been carried out to get a functional form of computed field (see Fig. 2). Hence, a correcting field map function $w(x,z)$ may be defined as

$$w(x,z) = \begin{cases} f_i(x) & \text{if } z \text{ is in block } i \text{ of the F half-unit} \\ 1 & \text{otherwise} \end{cases}$$

where $f_i(x)$ is the ratio of the computed field function on shimmed block i over the corresponding function derived without shim insertion.

Multiplying the measured field map values by $w(x,z)$ yields the field map relevant for the stray field in the presence of shims, which is of importance for good extraction modeling.

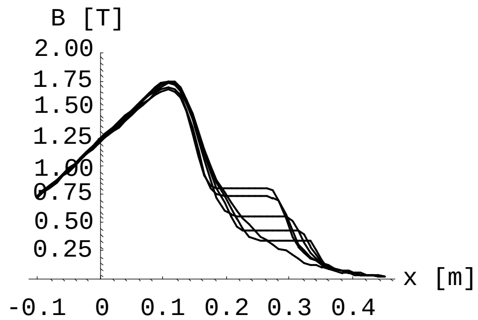

Fig. 2: Calculated fields for the five shimmed and un-shimmed blocks over the range -0.1 m ≤ x ≤ 0.5 m.

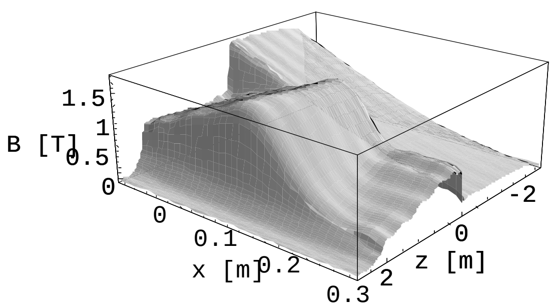

Fig. 3: Fitted field map for the 26 GeV/c working point after mixing of the shim model into the measured data.

Least squares fit of the discrete field map after mixing of the shim model has been performed using two-dimensional polynomials to get a functional form $B_y(x,z)$ which can be handled by the differential equations for the betatron motion. Polynomials up to degree fourteen in x and z have been retained to reach a good agreement with the measured field (accuracy within ±0.01 T). The fitting was performed using the standard *Mathematica* fit function [6] (see Fig. 3).

3. BEAM PATH, TRANSFER MATRIX

The radial centroid motion of the beam in any field $B_y(x,z)$ expressed in a Cartesian frame is given by the non-linear differential system [7]

$$\frac{dx}{dz} = \tan\phi \qquad \frac{d(\sin\phi)}{dz} = -\frac{e}{p} B_y$$

where x and ϕ are the trajectory's position and angle.

Small deviations ξ, ψ, Δp (respectively η, χ) in position, angle and momentum about the horizontal (respectively vertical) particle trajectory are given by the linear system

$$\frac{d\xi}{dz} = \frac{\psi}{\cos^2\phi} \qquad \frac{d(\psi\cos\phi)}{dz} = -K_x\xi + \frac{1}{\rho}\frac{\Delta p}{p}$$

$$\frac{d\eta}{dz} = \frac{\chi}{\cos\phi} \qquad \frac{d\chi}{dz} = (K_x - K_z\tan\phi)\eta$$

where ρ is the local curvature radius and K_x, K_z are the normalized strengths defined as

$$K_x = \frac{e}{p}\frac{dB_y}{dx} \qquad K_z = \frac{e}{p}\frac{dB_y}{dz}$$

Solutions of the linear system may be expressed as a transfer matrix from the field map entrance to its exit. In the horizontal plane the change of variables $q=\xi\cos\phi$ is required for the determinant of the transfer matrix to be unity.

4. BEAM PARAMETERS

The CPS and the TT2 transport channel which links it to the SPS have been modeled using the MAD program [8]. The 26 GeV/c proton ejection process begins with CPS optics calculation (including a local orbit deformation at the ejection septum and the kick of the ejection kicker), follows by the transport through the stray field (i.e. from ejection septum exit), and ends with the TT2 transfer line optics calculation [9]. Ejection trajectory, shown on Fig. 4, and transfer matrix computations through the magnet stray field have been performed using the built-in *Mathematica* numerical differential equation solver with initial conditions given by MAD.

The beam centroid enters the field map with coordinates x=91.6 mm, ϕ=62.6 mrad, and exits the field map at x=345.0 mm, ϕ=36.4 mrad. For comparison the angle of the ejection pipe with respect to the z-axis in the F half-unit number 16 is 43 mrad. Calculation of the transfer matrices using the above linear system (with different values of q, ψ, $\Delta p/p$ for the horizontal plane and η, χ for the vertical plane) yields:

$$\begin{pmatrix} q \\ \psi \\ \frac{\Delta p}{p} \end{pmatrix}_{\mathrm{out}} = \begin{pmatrix} 1.350 & 5.705 & 0.079 \\ 0.083 & 1.090 & 0.026 \\ 0 & 0 & 1 \end{pmatrix} \begin{pmatrix} q \\ \psi \\ \frac{\Delta p}{p} \end{pmatrix}_{\mathrm{in}}$$

$$\begin{pmatrix} \eta \\ \chi \end{pmatrix}_{\mathrm{out}} = \begin{pmatrix} 0.665 & 4.878 \\ -0.081 & 0.909 \end{pmatrix} \begin{pmatrix} \eta \\ \chi \end{pmatrix}_{\mathrm{in}}$$

The determinants of these matrices are not exactly equal to unity because the *Mathematica* numerical equation solver is not symplectic.

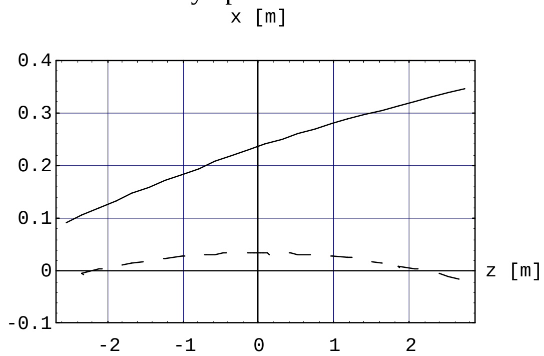

Fig. 4: Ejection (solid line) and central trajectories (dotted line) through the field map.

5. RESULTS AND CONCLUSION

5.1 Comparison with the previous model

The optical parameters have been derived from the above transfer matrix [7] and compared with previous models which consider the MAD stray field description given by dipole, quadrupole and sextupole coefficients distributed over the magnet length [9]. Both results, which agree reasonably well, are shown in Table 1.

	β_x *[m]*	α_x	D_x *[m]*	D_x'	β_y *[m]*	α_y
Field map	31.25	-2.71	3.10	0.26	7.11	0.74
MAD model	33.79	-3.37	3.25	0.32	6.13	0.85

Table 1: Optical parameters at the exit of the stray field.

5.2 Experimental verification

Optical parameters from the obtained field map at the location of SEM-grid beam profile detectors in the TT2 transport channel are shown in table 2.

SEM-grid location	β_x *[m]*	α_x	D_x *[m]*	D_x'	β_y *[m]*	α_y
MSG 257	13.31	1.14	0.90	-0.21	27.19	-1.20
MSG 267	10.99	0.20	-1.41	-0.07	32.25	-1.71
MSG 277	23.07	0.94	-2.51	0.12	42.05	-2.03

Table 2: Optical parameters at the three beam profile detectors in the CPS-SPS transfer channel (TT2).

Transverse emittance matching in the TT2 transfer channel is obtained from beam profiles measured at three SEM-grid detectors. Using the optical parameters in Table 2, the mismatch derived from measurements [10] was found to be less than 15% for the horizontal plane (see Fig. 5) and less than 10% for the vertical plane. This is a fairly good result (the best achieved so far) considering that an error on optical parameters transforms into a large mismatch error. More studies will be carried out on the present ejected proton beam trajectories to further improve the knowledge of the matching.

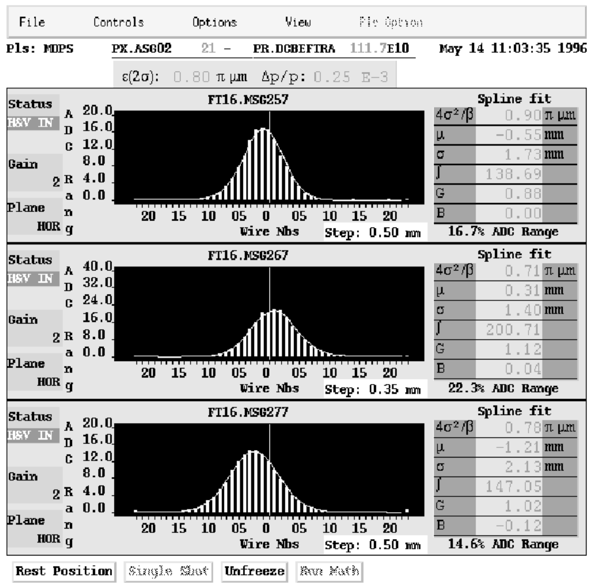

Fig. 5: Beam profile, matching and emittance measurements in the PS-SPS transfer channel.

6. ACKNOWLEDGMENTS

The authors wish to thank B. Autin, R. Cappi, D. Cornuet, E. Métral, T. Risselada, J.P. Riunaud and J.M. Roux for stimulating discussions on the subject.

REFERENCES

[1] The LHC Study Group, "The Large Hadron Collider, Conceptual Design", CERN/AC/95-05 (LHC).

[2] D. Cornuet, Z. Sharifullin, "Magnetic Measurements on the PS Magnet Unit U17 with Hall Probes", CERN technical note AT/MA Note 92-23.

[3] P. Bossard, "Shim for Ejection 16", MPS/SI/Note MAE/68-8, 1968.

[4] K. Halbach, "A Program for Inversion of System Analysis and its Application to the Design of Magnets", Proc 2nd Conf. On Magnet Technology, Oxford, England, 1967.

[5] E. Métral "Modélisation d'une Ligne de Transport de Faisceaux", to be published.

[6] S. Wolfram, "Mathematica, A System for Doing Mathematics by Computer", Addisson-Wesley, 1991.

[7] B. Autin, "Introduction to Beam Optics", CERN/PS/84-18 (AA), 1984.

[8] H. Grote, F.Iselin, "The MAD program, Version 8.19", http://hpariel.cern.ch/fci/mad/mad.html.

[9] T. Risselada, "Beam Optics Data for the PS Ring and its Transfer Lines", PS-PA Note 92-04.

[10] M. Arruat, M. Martini, "The New Standard Method to Measure Emittances in the PS Transfer Lines", CERN/PS 92-59 (PA).